

Document downloaded from:

<http://hdl.handle.net/10251/148463>

This paper must be cited as:

Juarez, LA.; Costero, AM.; Parra Alvarez, M.; Gaviña, P.; Gil Grau, S.; Martínez-Máñez, R.; Sancenón Galarza, F. (2017). NO₂-controlled cargo delivery from gated silica mesoporous nanoparticles. *Chemical Communications*. 53(3):585-588.
<https://doi.org/10.1039/c6cc08885f>



The final publication is available at

<https://doi.org/10.1039/c6cc08885f>

Copyright The Royal Society of Chemistry

Additional Information

NO₂-controlled cargo delivery from gated silica mesoporous nanoparticles

Received 00th January 20xx,
Accepted 00th January 20xx

L. Alberto Juárez,^{a,b,c} Ana M. Costero,^{a,b,c,*} Margarita Parra,^{a,b,c} Pablo Gaviña,^{a,b,c} Salvador Gil,^{a,b,c} Ramón Martínez-Máñez^{a,b,d,*} and Félix Sancenón^{a,b,d}

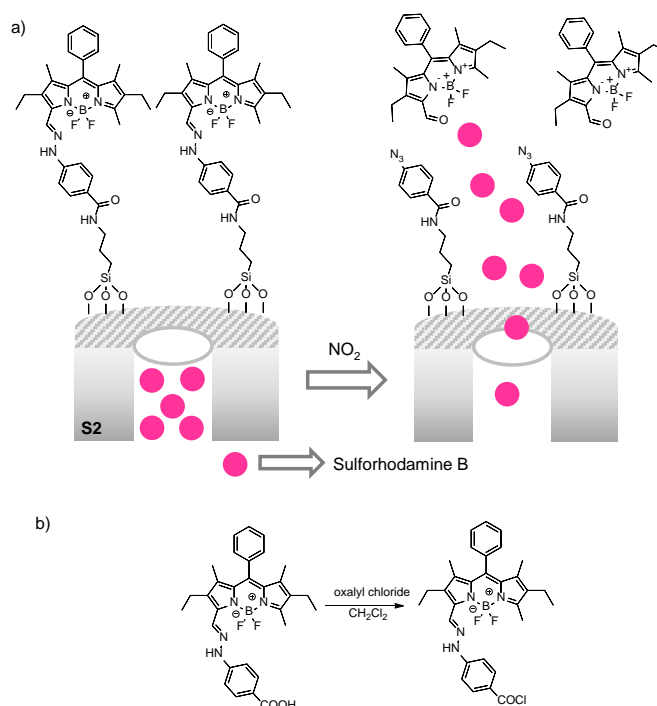
DOI: 10.1039/x0xx00000x

www.rsc.org/

Cargo delivery from mesoporous silica nanoparticles loaded with sulforhodamine B and capped with a difluorboron-dipyrromethene (BODIPY) derivative was triggered by an NO₂-induced oxidative process.

Stimuli-responsive nanomaterials, able to show a switchable behavior in response to environmental changes, are novel smart systems with promising applications.^{1,2} One appealing use of such materials is the design of functionalized nanocontainers able to release an entrapped cargo under controlled conditions via external triggers.³ Traditional delivery systems usually rely on simple diffusion controlled processes or degradation of the nanocarrier,⁴ using for instance microcapsules,⁵ micelles,⁶ vesicles,⁷ or liposomes.⁸ As an alternative to these soft nanomaterials, the use of mesoporous silica nanoparticles (MSNs) as inorganic scaffoldings for the development of controlled delivery systems has attracted great concern in the last years. MSNs have unique properties such as large surface area (up to 1200 m² g⁻¹), the presence of tunable pore sizes with diameters in the 2-10 nm range, high load capacity, biocompatibility, high thermal stability, inertness and easy functionalization using well-known alkoxy silane-based chemistries.⁹ In this scenario, several examples of MSNs containing capping molecular/supramolecular assemblies and able to be opened or closed at will upon application of selected stimuli have recently been described.¹⁰ The use of light, temperature, alternating magnetic fields, ultrasounds, pH, redox, enzymes and molecules/biomolecules, etc. as external stimuli has been described.^{10,11} These gated MSNs were initially developed as

potential carriers for controlled drug delivery and have recently been also used in the design of advanced new sensing protocols.¹²



Scheme 1. (a) Schematic representation of capped S2 nanoparticles and (b) synthesis of BODIPY derivative 2.

These gated MSNs are usually obtained by anchoring certain binding or reactive sites onto the external surface of the inorganic support. Reaction or coordination of selected molecules with the grafted binding sites govern payload release. Based in this concept a variety of anions, cations, neutral molecules and biomolecules have been described to acts as triggers for payload delivery in MSNs.¹³ However, there are very few examples of capped materials able to cargo released in the presence of small neutral gaseous species. In

^a Instituto Interuniversitario de Investigación de Reconocimiento Molecular y Desarrollo Tecnológico (IDM). Universitat Politècnica de Valencia, Universitat de Valencia, Spain.

^b CIBER de Bioingeniería, Biomateriales y Nanomedicina (CIBER-BBN).

^c Departamento de Química Orgánica, Universitat de Valencia, Doctor Moliner 50, 46100, Burjassot, Valencia, Spain. E-mail: ana.costero@uv.es

^d Departamento de Química, Universidad Politècnica de Valencia, Camino de Vera s/n, 46022, Valencia, Spain. E-mail: rmaez@qim.upv.es

Electronic Supplementary Information (ESI) available: Synthesis and characterization of the prepared materials. See DOI: 10.1039/x0xx00000x

this scenario, the research groups of Lu and Bein used singlet oxygen (generated by photosensitizer irradiation) as trigger to induce release of certain dyes or drugs from polymer and liposome capped MSNs.¹⁴ Moreover, Ronconi and coworkers prepared MSNs loaded with rhodamine B and capped with an inclusion complex formed between a grafted ferrocene derivative and β -cyclodextrins that was opened in the presence of oxygen.¹⁵ However, in spite of these examples, the development of gated materials triggered by gaseous species is still a barely explored field.

Taking into account the above mentioned facts and our interest in the implementation of new opening mechanisms in gated materials^{10,16} we explored here the use of NO₂ as trigger. NO₂ has direct and indirect adverse health effects. Thus, NO₂ exposure is a potential inducer of neurological diseases.¹⁷ In addition, long-term exposure to NO₂ is associated with increased susceptibility to lower respiratory tract illness¹⁸ and increased risk of chronic obstructive pulmonary disease mortality.¹⁹

We report herein the preparation of a capped material based in MSNs as inorganic scaffold, loaded with sulforhodamine B and capped with a difluoroboron-dipyrromethene (BODIPY) derivative anchored to the mesoporous material through a hydrazone bond (**S2** solid in Scheme 1). The opening mechanism takes advantage of the NO₂ induced oxidative regeneration of carbonyl compounds from the corresponding hydrazones under very soft conditions.²⁰ This oxidative cleavage detached a BODIPY aldehyde from the nanoparticles surface with subsequent pore opening and cargo release. NO₂-triggered opening of **S2** nanoparticles can be followed not only by the emission of sulforhodamine B released from the pores but also by monitoring the fluorescence of the detached BODIPY aldehyde.

MCM-41 silica mesoporous nanoparticles were synthesized through well-known procedures using TEOS as the hydrolysable inorganic precursor and the surfactant *n*-cetyltrimethylammonium bromide.²¹ Then, pores of the calcined mesoporous scaffold were loaded with sulforhodamine B by simply stirring a suspension of the nanoparticles in an acetonitrile solution of the dye (solid **S0**). In a second step, the external surface of the loaded nanoparticles was functionalized with (3-aminopropyl) triethoxysilane yielding solid **S1**. Finally, solid **S2** was obtained by the reaction of hydrazone-containing BODIPY derivative **2** with the aminopropyl moieties on the surface of **S1**. **2** was obtained from **1** upon treatment with thionyl chloride (see Scheme 1 and Supporting Information for further information).²²

Starting silica mesoporous nanoparticles and solid **S2** were characterized following standard procedures (see Supporting Information for details). Powder X-ray diffraction (PXRD) and transmission electron microscopy (TEM), carried out on the starting MCM-41 mesoporous nanoparticles, clearly showed the presence of a mesoporous structure that persisted in solid **S2** regardless of the loading process with sulforhodamine B and further functionalization with **2** (see Figure 1). From thermogravimetric and elemental analyses, sulforhodamine B

(0.29 mmol/g SiO₂) and **2** (0.11 mmol/g SiO₂) contents were determined. Table 1 lists the main structural properties (BET specific surface area, pore volumes and pore sizes) for the starting MSNs and **S2** obtained from the N₂ adsorption-desorption measurements (see Supporting Information). As could be seen in Table 1 a remarkable decrease in specific surface area, pore volume and pore size of solid **S2**, compared with that of the MCM-41 starting material, was observed. These decreases are ascribed to the loading of the pores of MCM-41 scaffold with sulforhodamine B and subsequent grafting of the bulky BODIPY derivative **2**. The size of the prepared nanoparticles was assessed by TEM images, which gave an average particle diameter of 94.5 nm (see Figure 1).

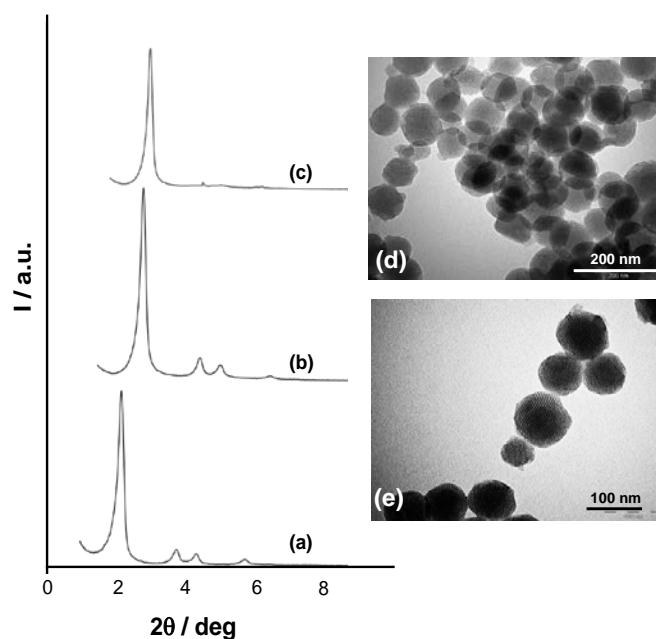


Figure 1. Left: PXRD patterns of the solids (a) MCM-41 as-synthesized, (b) calcined MCM-41 and (c) solid **S2**. Right: TEM images of (d) calcined MCM-41 and (e) solid **S2** showing the typical hexagonal porosity of the MCM-41 mesoporous matrix.

Table 1. BET-specific surface values, pore volumes and pore sizes calculated from the N₂ adsorption-desorption isotherms for selected materials.

Sample	S _{BET} [m ² g ⁻¹]	BJH pore ^[a,b] [nm]	Total pore volume ^[a] [cm ³ g ⁻¹]
MCM-41	895	2.97	0.73
S2	235	2.11	0.17

[a] Pore volumes and pore sizes were associated with only intraparticle mesopores. [b] Pore size estimated by the BJH model applied to the adsorption branch of the isotherm.

Once characterized, the response of **S2** nanoparticles was tested in the absence and in the presence of NO₂ by monitoring the release of the entrapped sulforhodamine B from **S2** ($\lambda_{\text{ex}} = 520$ nm, $\lambda_{\text{em}} = 570$ nm). Moreover, the course of pore opening can also be monitored by measuring the emission (at 530 nm) of the BODIPY aldehyde generated after reaction with NO₂ ($\lambda_{\text{ex}} = 520$ nm).

In a typical experiment, 1 mg of solid **S2** was suspended in 3 mL of acetonitrile in the absence of NO_2 . As could be seen in Figure 2 a negligible release of the entrapped sulforhodamine B was observed. However, when NO_2 (1 ppm) was bubbled in the suspension of **S2** a remarkable sulforhodamine B release was found. At the same time, an increase in the emission intensity at 530 nm was observed which was ascribed to the BODIPY aldehyde generated after the NO_2 -induced oxidative cleavage of the hydrazone bond in the molecular gate in **S2**. Moreover, release of BODIPY aldehyde to the solution was faster than that observed for sulforhodamine B because the former fluorophore was located in the outer surface of **S2** whereas the latter should diffuse from the inner pores of the inorganic scaffold (see Figure 2).

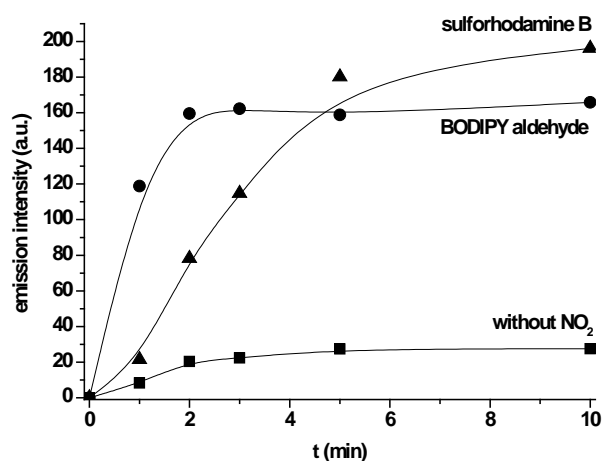


Figure 2. Sulforhodamine B ($\lambda_{\text{em}} = 570$ nm, $\lambda_{\text{ex}} = 520$ nm) and BODIPY aldehyde ($\lambda_{\text{em}} = 530$ nm, $\lambda_{\text{ex}} = 520$ nm) delivery profiles from **S2** nanoparticles in the absence and in the presence of NO_2 (1 ppm).



Figure 3. Visual changes observed for **S2** suspensions in acetonitrile before and after exposure to 0.25 and 0.5 ppm of NO_2 gas (from left to right). The picture shows the color of the corresponding acetonitrile solutions after elimination of the nanoparticles by centrifugation.

Besides, a clear color change from colorless to magenta was observed when NO_2 was bubbled onto **S2** acetonitrile suspension due to sulforhodamine B and BODIPY aldehyde release (see Figure 3). These color changes can be observed by naked-eye and suggest a possible application of **S2** for sensing the presence of NO_2 in air.

From titration studied of **S2** in the presence of NO_2 , it was found that cargo delivery can be observed at concentration of NO_2 as low as 0.11 ppm. This value is lower than the alarm threshold of $400 \mu\text{g m}^{-3}$ (ca. 0.2 ppm) established by the European Union for nitrogen dioxide.²³ In a final step, the response of **S2** in the presence of other gases (i.e. NO , CO_2 , H_2S , SO_2), in concentrations up to 100 ppm, was also studied.

Moreover, the nanoparticles were tested when bubbling air-containing vapours of acetone, hexane, chloroform, acetonitrile and toluene (up to 100 ppm in air) to acetonitrile solutions of **S2**. As could be seen in Figure 4 a very poor cargo delivery (nor BODIPY detachment from the surface) was observed in the presence of these gases when compared with payload delivery found in the presence of NO_2 .²⁴

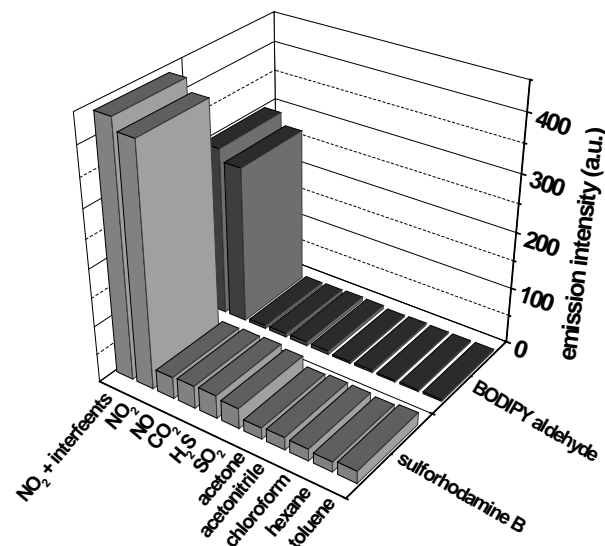


Figure 4. Emission intensity of sulforhodamine B (570 nm) and BODIPY aldehyde (530 nm) released from acetonitrile suspensions of **S2** nanoparticles in the presence of NO_2 , gases (NO , CO_2 , H_2S , SO_2) and organic vapours (acetone, hexane, chloroform, acetonitrile, toluene) at 100 ppm. In all cases, dye released was monitored upon bubbling air containing the corresponding gas to acetonitrile suspensions of **S2**.

In summary, we have prepared mesoporous nanoparticles capped with a hydrazone-containing BODIPY derivative that were selectively opened in the presence of NO_2 gas. NO_2 induced the oxidative cleavage of the hydrazone linkage BODIPY capping molecules, inducing pore opening and delivery of entrapped sulforhodamine B. Cargo delivery from the capped **S2** material was only observed in the presence of NO_2 , whereas other gases (such as NO , CO_2 , H_2S , SO_2) or vapours of typical organic solvents were unable to open the gated ensemble. As far as we know this is the first gated material able to be opened in the presence of NO_2 and it is one of the few examples described in which delivery from gated ensembles is induced by the presence of a gas molecule.

The authors thank the financial support from the Spanish Government (project MAT2015-64139-C4-R) and the Generalitat Valenciana (project GVA/2014/13).

References

- 1 K. Ariga, A. Vinu, J. P. Hill, T. Mori, *Coord. Chem. Rev.*, 2007, **251**, 2562.

- 2 E. Katz, I. Willner, *Angew. Chem. Int. Ed.*, 2004, **43**, 6042.
- 3 A. B. Descalzo, R. Martínez-Máñez, F. Sancenón, K. Hoffmann, K. Rurack, *Angew. Chem. Int. Ed.*, 2006, **45**, 5924.
- 4 (a) F. Puoci, F. Iemma, N. Picci, *Curr. Drug Deliver.*, 2008, **5**, 85. (b) F. Siepmann, J. Siepmann, M. Walther, R. MacRae, R. Bodmeier, *J. Control. Release*, 2008, **125**, 1.
- 5 M. Hamidi, A. Azadi, P. Rafiei, *Adv. Drug Deliver. Rev.*, 2008, **17**, 1638.
- 6 C. W. Pouton, C. J. H. Porter, *Adv. Drug Deliver. Rev.*, 2008, **17**, 625.
- 7 C. J. F. Rijcken, O. Soga, W. E. Hennink, C. F. van Nostrum, *J. Control. Release*, 2007, **120**, 131.
- 8 T. L. Andresen, S. S. Jensen, K. Jorgensen, *Prog. Lipid Res.*, 2005, **44**, 69.
- 9 (a) J. S. Beck, J. C. Vartuli, W. J. Roth, M. E. Leonowicz, C. T. Kresge, K. D. Schmitt, C. T. –W. Chu, D. H. Olson, E. W. Sheppard, S. B. McCullen, J. B. Higgins, J. L. Schlenker, *J. Am. Chem. Soc.*, 1992, **114**, 10834. (b) A. P. Wright, M. E. Davis, *Chem. Rev.*, 2002, **102**, 3589. (c) G. Kickelbick, *Angew. Chem., Int. Ed.*, 2004, **43**, 3102. (d) A. Stein, *Adv. Mater.*, 2003, **15**, 763.
- 10 (a) E. Aznar, M. Oroval, Ll. Pascual, J. R. Murguía, R. Martínez-Máñez, F. Sancenón, *Chem. Rev.*, 2016, **116**, 561. (b) G. J. A. A. Soler-Illia, O. Azzaroni, *Chem. Soc. Rev.*, 2011, **40**, 1107.
11. (a) S. Saha, K. C. F. Leung, T. D. Nguyen, J. F. Stoddart, J. I. Zink, *Adv. Func. Mater.*, 2007, **17**, 685. (b) F. Wang, X. Liu, I. Willner, *Angew. Chem. Int. Ed.*, 2015, **56**, 1098. (c) N. Song, Y. –W. Yang, *Chem. Soc. Rev.*, 2015, **44**, 3474. (d) B. G. Trewyn, S. Giri, I. I. Slowing, V. S. –Y. Lin, *Chem. Commun.*, 2007, 3236.
12. F. Sancenón, Ll. Pascual, M. Oroval, E. Aznar, R. Martínez-Máñez, *ChemistryOpen*, 2015, **4**, 418.
- 13 See for example: (a) R. Casasús, E. Aznar, M. D. Marcos, R. Martínez-Máñez, F. Sancenón, J. Soto, P. Amorós, *Angew. Chem. Int. Ed.*, 2006, **45**, 6661. (b) C. Coll, R. Casasús, E. Aznar, M. D. Marcos, R. Martínez-Máñez, F. Sancenón, J. Soto, P. Amorós, *Chem. Commun.*, 2007, 1957. (c) V. C. Ozalp, T. Schafer, *Chem. Eur. J.*, 2011, **17**, 9893. (d) E. Climent, M. D. Marcos, R. Martínez-Máñez, F. Sancenón, J. Soto, K. Rurack, P. Amorós, *Angew. Chem. Int. Ed.*, 2009, **48**, 8519. (e) Y. Wen, L. Xu, C. Li, H. Du, L. Chen, B. Su, Z. Zhang, X. Zhang, Y. Song, *Chem. Commun.*, 2012, **48**, 8410. (f) Z. Zhang, D. Balogh, F. A. Wang, I. Willner, *J. Am. Chem. Soc.*, 2013, **135**, 1934. (g) Y. Zhou, L. –L. Tan, Q. –L. Li, X. –L. Qiu, A. –D. Qi, Y. Tao, Y. –W. Yang, *Chem. Eur. J.*, 2014, **20**, 2998. (h) M. Chen, C. Huang, C. He, W. Zhu, Y. Xu, Y. Lu, *Chem. Commun.*, 2012, **48**, 9522. (i) E. Climent, A. Bernardos, R. Martínez-Máñez, A. Maquieira, M. D. Marcos, N. Pastor-Navarro, R. Puchades, F. Sancenón, J. Soto, P. Amorós, *J. Am. Chem. Soc.*, 2009, **131**, 14075.
- 14 (a) S. Yang, N. Li, Z. Liu, W. Sha, D. Chen, Q. Xu, J. Lu, *Nanoscale*, 2014, **6**, 14903. (b) A. Schlossbauer, A. M. Sauer, V. Cauda, A. Schmidt, H. Engelke, U. Rothbauer, K. Zolghadr, H. Leonhardt, C. Bräuchle, T. Bein, *Adv. Healthcare Mater.*, 2012, **1**, 316. (c) S. A. Mackowiak, A. Schmidt, V. Weiss, C. Argyo, C. von Schirnding, T. Bein, C. Bräuchle, *Nano Lett.*, 2013, **13**, 2576.
- 15 G. Q. Silveira, M. D. Vargas, C. M. Ronconi, *J. Mater. Chem.*, 2011, **21**, 6034.
- 16 See for example: (a) C. Coll, A. Bernardos, R. Martínez-Máñez, F. Sancenón, *Acc. Chem. Res.*, 2013, **46**, 339. (b) S. El Sayed, M. Milani, C. Milanese, M. Licchelli, R. Martínez-Máñez, F. Sancenón, *Chem. Eur. J.*, 2016, **22**, 13935. (c) C. de la Torre, I. Casanova, G. Acosta, C. Coll, M. J. Moreno, F. Albericio, E. Aznar, R. Mangues, M. Royo, F. Sancenón, R. Martínez-Máñez, *Adv. Func. Mater.*, 2015, **25**, 687. (d) C. Giménez, E. Climent, E. Aznar, R. Martínez-Máñez, F. Sancenón, M. D. Marcos, P. Amorós, K. Rurack, *Angew. Chem. Int. Ed.*, 2014, **53**, 12629. (e) E. Climent, L. Modragón, R. Martínez-Máñez, F. Sancenón, M. D. Marcos, J. R. Murguía, P. Amorós, K. Rurack, E. Pérez-Payá, *Angew. Chem. Int. Ed.*, 2013, **52**, 8938.
- 17 H. Li, L. Chen, Z. Guo, N. Sang, G. Li, *J. Hazard. Mater.*, 2012, **225**, 46.
- 18 (a) L. J. Folinsbee, *Environ. Health Perspect.*, 1992, **100**, 45. (b) R. J. W. Melia, C. Florey, D. G. Altman, A. V. Swan, *Br. Med. J.*, 1977, **2**, 149. (c) L. M. Neas, D. W. Dockery, J. D. Spengler, F. E. Speizer, B. G. Ferris, *Am. J. Epidemiol.*, 1991, **134**, 204.
- 19 X. Meng, C. Wang, D. Cao, C. M. Wong, H. Kan, *Atmos. Environ.*, 2013, **77**, 149.
- 20 (a) S. B. Shim, K. Kim, J. H. Kim, *Tetrahedron Lett.*, 1987, **28**, 645. (b) J. Mokhtari, M. R. Naimi-Jamal, H. Hamzeali, M. G. Dekamin, G. Kaupp, *ChemSusChem*, 2009, **2**, 248.
- 21 (a) S. Cabrera, J. El. Haskouri, C. Guillem, J. Latorre, A. Beltrán, D. Beltrán, M. D. Marcos P. Amorós, *Solid State Sci.*, 2000, **2**, 405. (b) D. R. Radu, C. –Y. Lai, K. Jeftinija, E. W. Rowe, S. Jeftinija V. S. –Y. Lin, *J. Am. Chem. Soc.*, 2004, **126**, 13216.
- 22 L. A. Juárez, A. M. Costero, M. Parra, P. Gaviña, S. Gil, *Chem. Eur. J.* **2016**, **22**, 8448.
- 23 European Commission (accessed February 2016), <http://ec.europa.eu/environment/air/quality/standards.html>
24. Experiments with ozone were carried out due to it had been established that ozone was able to regenerate carbonyl groups from their corresponding hydrazones. However, under these conditions both sulforhodamine B and the generated aldehyde react with the ozone giving rise to a colorless solution.